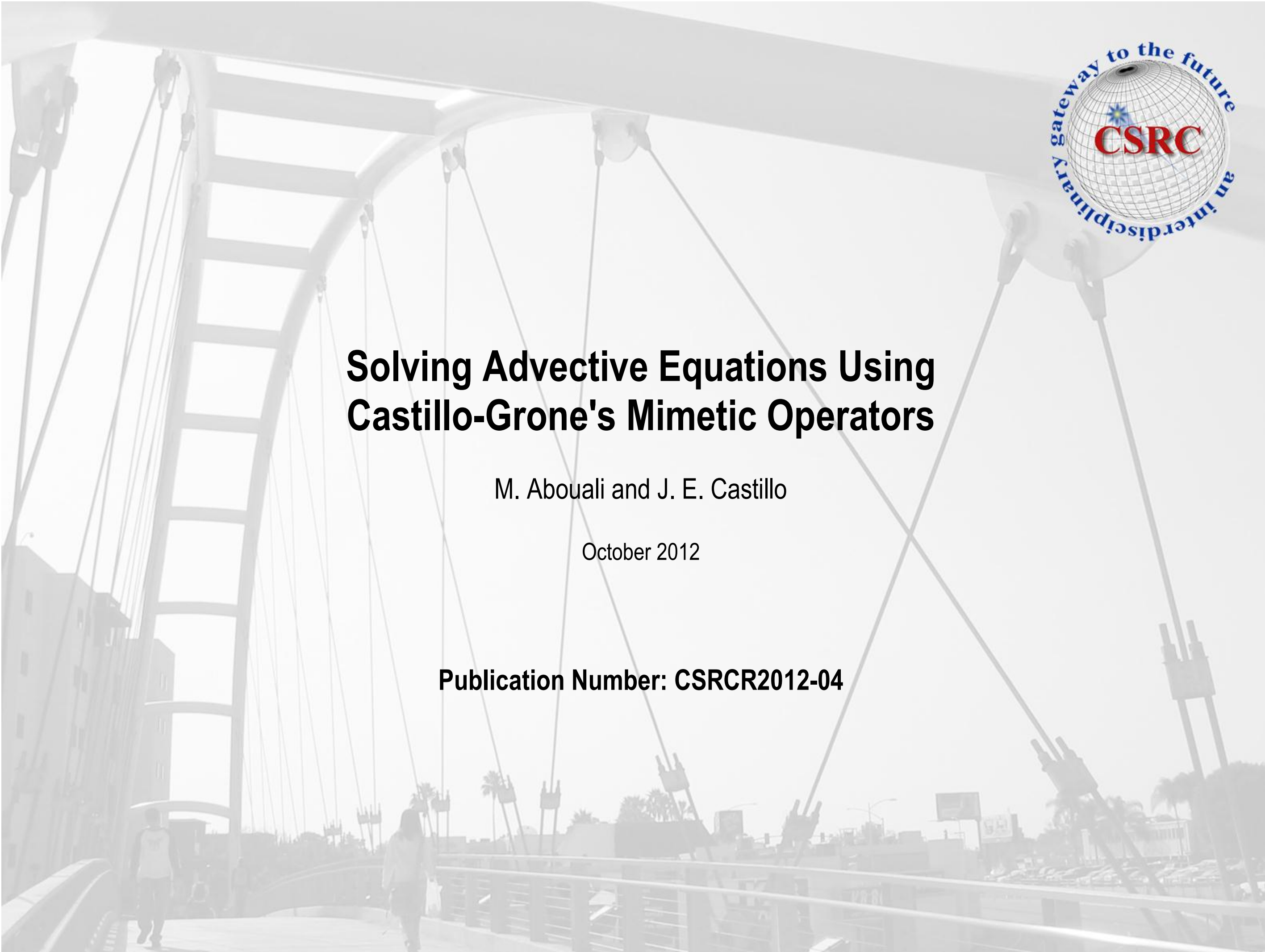

Solving Advective Equations Using Castillo-Grone's Mimetic Operators

M. Abouali and J. E. Castillo

October 2012

Publication Number: CSRCR2012-04

Computational Science &
Engineering Faculty and Students
Research Articles

Database Powered by the
Computational Science Research Center
Computing Group & Visualization Lab

COMPUTATIONAL SCIENCE & ENGINEERING

SAN DIEGO STATE UNIVERSITY

Computational Science Research Center
College of Sciences
5500 Campanile Drive
San Diego, CA 92182-1245
(619) 594-3430

Solving Advective Equations Using Castillo-Grone's Mimetic Operators

M. Abouali[a,b], J. E. Castillo[a,c]

[a] *Computational Science Research Center at San Diego State University, 5500 Campanile Drive, San Diego, CA 92182-1245, USA*
[b] *email: mabouali@mail.sdsu.edu*
[c] *email: castillo@myth.sdsu.edu,*
Phone: (+1) (619) 594-3430, Fax: (+1) (619) 594-2459

Abstract

In this paper, the performance of the second and forth order accurate Castillo-Grone's Mimetic Gradient and Divergence operator for solving the advection equation along with RK3 time discretization scheme is investigated. Also, the effect of interpolation on these operators is studied. It was shown that in all cases the CGM operators where stable for Courant number above 1 and in some cases upto Courant number 1.8.

Keywords: Castillo-Grone's Mimetic Operators, High-Order Operators, Advection Equation, Time-Split Scheme, RK3, Interpolation

1. Introduction

Both hydrostatic and nonhydrostatic ocean and atmosphere models deal with different scales of the motions and forces with wide range of frequencies. A shorter time step is required for high-frequency features while a larger time step can be chosen for low-frequency ones. Hence, in order to address the wide range of frequencies with a single time step, it is very common to use a time-splitting method in these models [1]. There are various explicit time-splitting scheme available. Klemp and Wilhelmson combined leapfrog and a forward-backward scheme [2] to derive perhaps one of the most commonly used scheme back in 1978 [3]. Crowley scheme is another splitting method for time integration [4]. Wicker and Skamarock have introduced several versions of their time-split scheme based on a two-step Runge-Kutta method (RK2) [5] and third-order Runge-Kutta method (RK3). Wicker and Skamarock has shown the superiority of their RK3 scheme in time integration [6]. The accuracy, efficiency, and ease of implementation of their proposed RK3 scheme have motivated the authors in this paper to use the same time-splitting scheme in the Unified Curvilinear Ocean Atmosphere Model (UCOAM) [7]. It is note worthy to mention that RK3 is also currently being used in the Weather Research & Forecasting (WRF) Model, the most commonly used model in the field [8, 9].

However, time integration is only one side of the coin. Other factors that affect the stability in elastic models and advective equations are (1) the spatial discretization [10, 11, 12] and (2) the interpolation schemes [6]. Particularly, the combination of the spatial discretization and the time integration is very important. Some spatial discretization schemes become unstable with certain time discretization schemes, while changing the time discretization and keeping the same spatial discretization may alleviate the problem. As an example, a central spatial scheme is unconditionally unstable with RK2 or Euler method [11]. It is also widely known that in general, increasing the order of accuracy will limit the stability regions in many cases; hence, a much smaller time step needs to be selected [11].

Interpolation also has the same effect. While higher order interpolation schemes are more accurate, they will limit the stability region. As an example, Wicker and Skamarock has shown that their RK3 scheme along with a second order accurate central finite-volume scheme is sensitive to the interpolation scheme in use, as the stable Courant number decreases from 1.61 to 1.08 by increasing the order of accuracy of the interpolator function from three to six [6].

This paper extends the work of Wicker and Skamarock [6] by investigating the performance of the Castillo-Grone's Mimetic (CGM) difference operators with higher order of accuracies. Mimetic schemes are a class of numerical schemes that satisfy the physical properties of their continuous operator in discrete environment [13, 14, 15, 16, 17, 18, 19]. It has to be noted that the second order central finite-volume scheme used in the paper by Wicker and Skamarock is also categorized as a mimetic scheme. In this paper, 4th order CGM divergence and gradient operator along with first, forth and sixth order accurate interpolation methods are tested and their performance is reported. The reason to consider first order accurate linear interpolation comes from the authors' interest in using NVIDIA's Graphical Processing Units (GPUs). GPUs have special circuitry for one, two, and three dimensional linear/bilinear/ trilinear interpolation. Therefore, the interpolation can be done very efficiently and fast at the hardware level. Although, the same circuitry can be harnessed for higher order interpolation schemes with a little bit of help on the software side.

Next section covers the governing equations, the test function, initial and boundary conditions, RK3 scheme, CGMimetic operators, Kawamura approach, and the interpolation schemes. Later the results of each method is presented and the region of stability is discussed based on the stable Courant number.

2. Numerical Approach

2.1. Governing Equation

The advection equation in the absence of any source or sink term can be formulated in non-conservative form using the gradient operator, as follows:

$$\frac{\partial q}{\partial t} + u \cdot \bigtriangledown(q) = 0 \tag{1}$$

where q is a scalar quantity, which is advected by the velocity field, i.e. u. Remembering that $\bigtriangledown \cdot (uq) = u \cdot \bigtriangledown(q) + q(\bigtriangledown \cdot u)$ and using the continuity equation, which for incompressible fluids can be written as $\bigtriangledown \cdot u = 0$, equation (1) can be written in conservative form using the divergence operator as follows:

$$\frac{\partial q}{\partial t} + \bigtriangledown \cdot (uq) = 0 \tag{2}$$

In this paper both forms of the equation are investigated. The CGM gradient operator is used with equation (1) and CGM divergence operator is used with equation (2).

2.2. Initial and Boundary Conditions

q is initialized with:

$$q(x, t = 0) = \frac{1}{1 + e^{|80(z-0.15)|}}, \tag{3}$$

where $z = |x - 0.5|$ and $x \in [0, 1]$. A periodic boundary condition is selected and the space discretization used $dx = 0.02$, dt is kept constant at 0.02, and u is chosen based on the given Courant number as follows:

$$u = \frac{C_r\ dx}{dt} \tag{4}$$

2.3. Spatial Discretization

2.3.1. KWM Scheme

Due to the nature of advective terms, it is widely believed that a forward or backward step works better for advective terms. Kawamura et al. [20] combined a forward and a backward scheme into a single equation in curvilinear coordinates. This scheme, abbreviated here as KWM, is forth order accurate and does not require any interpolation. Adapting the KWM scheme for the regularly spaced grids, the KWM scheme will look like:

$$\left(u\frac{\partial q}{\partial x}\right)_i = u_i\frac{-q_{i+2}+8(q_{i+1}-q_{i-1})+q_{i-2}}{12dx} + |u_i|\frac{q_{i+2}-4q_{i+1}+6q_i-4q_{i-1}+q_{i-2}}{4dx} \quad (5)$$

2.3.2. Castillo-Grone's Gradient and Divergence operators

The second order accurate Castillo-Grone's Mimetic (CGM) gradient operator is:

$$G_2 = \frac{1}{h}\begin{bmatrix} \frac{-8}{3} & 3 & \frac{-1}{3} & & \\ & -1 & 1 & & \\ & & -1 & 1 & \\ & & \frac{1}{3} & -3 & \frac{8}{3} \end{bmatrix}. \quad (6)$$

Likewise, the second order accurate CGM divergence operator is:

$$D_2 = \frac{1}{h}\begin{bmatrix} -1 & 1 & & & \\ & -1 & 1 & & \\ & & -1 & 1 & \\ & & & -1 & 1 \end{bmatrix}. \quad (7)$$

The forth order accurate CGM gradient and divergence operator are each part of a three parameter family of operators. Here, we use only one member of each families. The CGM divergence operator corresponding to the parameters, $(\alpha, \beta, \gamma) = (0, \frac{1}{24}, \frac{-1}{24})$ is:

$$D_4 = \frac{1}{h}\begin{bmatrix} \frac{-1045}{1142} & \frac{909}{1298} & \frac{201}{514} & \frac{-1165}{5192} & \frac{129}{2596} & \frac{-25}{15576} & & & & \\ \frac{1}{24} & \frac{-9}{8} & \frac{9}{8} & \frac{-1}{24} & & & & & & \\ & \frac{1}{24} & \frac{-9}{8} & \frac{9}{8} & \frac{-1}{24} & & & & & \\ & & & & \cdots & & & & & \\ & & & & & & \frac{1}{24} & \frac{-9}{8} & \frac{9}{8} & \frac{-1}{24} \\ & & & & \frac{25}{15576} & \frac{-129}{2596} & \frac{1165}{5192} & \frac{-201}{514} & \frac{-909}{1298} & \frac{1045}{1142} \end{bmatrix}. \quad (8)$$

Likewise, the chosen forth order CGM gradient operator is:

$$
G_4=\frac{1}{h}\begin{bmatrix}
\frac{-1775}{528} & \frac{1790}{407} & \frac{-2107}{1415} & \frac{1496}{2707} & \frac{-272}{2655} & \frac{25}{9768} & & & & \\
\frac{16}{105} & \frac{-31}{24} & \frac{29}{24} & \frac{-3}{40} & \frac{1}{168} & & & & & \\
 & \frac{1}{24} & \frac{-9}{8} & \frac{9}{8} & \frac{-1}{24} & & & & & \\
 & & \frac{1}{24} & \frac{-9}{8} & \frac{9}{8} & \frac{-1}{24} & & & & \\
 & & & & \cdots & & & & & \\
 & & & & & \frac{1}{24} & \frac{-9}{8} & \frac{9}{8} & \frac{-1}{24} & \\
 & & & & & \frac{-1}{168} & \frac{3}{40} & \frac{-29}{24} & \frac{31}{24} & \frac{-16}{105} \\
 & & & & \frac{-25}{9768} & \frac{272}{2655} & \frac{-1496}{2707} & \frac{2107}{1415} & \frac{-1790}{407} & \frac{1775}{528}
\end{bmatrix}. \quad (9)
$$

2.4. RK3 Scheme

In this paper a three steps time-split scheme introduced by Wicker and Skamarock [6] is used to integrate the equations provided in the form of:

$$
\frac{\partial u}{\partial t} = f(u, \cdots). \quad (10)
$$

To advance the solution for one step, i.e. integrating the equation to obtain u^{n+1} knowing the u^n, the following steps must be taken:

$$
\begin{aligned}
u^* &= u^n - \frac{dt}{3} f(u^n, \cdots) \\
u^{**} &= u^n - \frac{dt}{3} f(u^*, \cdots) \\
u^{n+1} &= u^n - \frac{dt}{3} f(u^{**}, \cdots)
\end{aligned} \quad (11)
$$

2.5. Fourth and Sixth Order Interpolation

On a regularly spaced grid, with spacing h, the forth order interpolation scheme can be written as follows:

$$q_{i-\frac{1}{2}} = \frac{7(q_i + q_{i-1}) - (q_{i+1} + q_{i-2})}{12}, \tag{12}$$

where q_i is located at $x_i = x_0 + i * h$. Likewise, the sixth order accurate interpolation can be written as follows:

$$q_{i-\frac{1}{2}} = \frac{37(q_i + q_{i-1}) - 8(q_{i+1} - q_{i-2}) + (q_{i+2} + q_{i-3})}{60}. \tag{13}$$

3. Results and Discussions

MATLAB was used to solve equation (1) and (2) numerically using the discretization schemes shown in previous sections. Periodic boundary condition were applied in all cases and the number of iterations were chosen in such a way that the initial signal passes through the domain twice and reaches its original position. Since the velocity is kept constant through out the space and time, in a perfect case one must get exactly the same signal. However, in practice due to numerical errors this will never happen. To measure the error the Root Mean Square Error (RMSE) was used.

The KWM scheme produced a very smooth and relatively accurate results. However, it was stable only upto a Courant number 0.6. Once $Cr > 0.63$ was chosen the scheme became unstable. The RMSE for this method stays relatively constant and does not change with increasing the Courant number. Hence, unlike other methods, there is no sign that this scheme is becoming unstable and just suddenly by increasing the Courant number the scheme is completely unstable. This is not a desirable behavior. Figure (1) shows the solution using Kawamura scheme.

The second order accurate CGM divergence operator also provided smooth results. Once a forth order interpolation scheme was used, the scheme was stable upto Courant number 1.3 and it was stable upto Courant number 1.1 for a sixth order interpolation scheme. However, the sixth order interpolation scheme resulted in more accuracy only at lower Courant numbers and once the Courant number reached 0.7 both methods were behaving more or less the same. In figure (2) and (3) the numerical solution is compared with the analytic solution using the second order CGM divergence operator with forth and sixth order interpolation scheme respectively.

Before discussing the results obtained using CGM gradient operator, it has to be reminded that the CGM gradient operator is developed for staggered meshes. CGM gradient operator requires the data to be in the middle of the cells and also on the

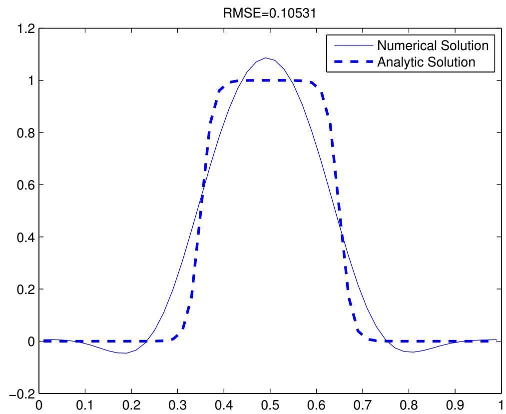

Figure 1: Kawamura Scheme with $Cr = 0.6$.

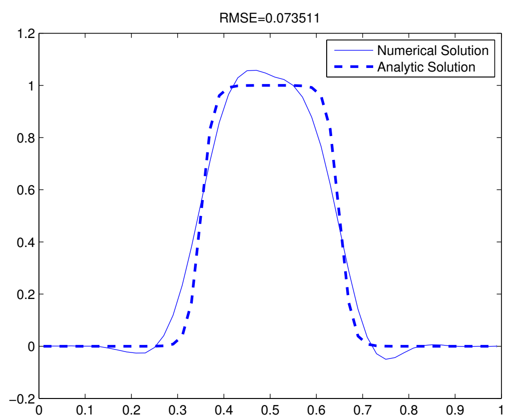

Figure 2: Second Order Accurate CGM Divergence Operator with Forth Order Interpolation Scheme, $Cr = 1.2$.

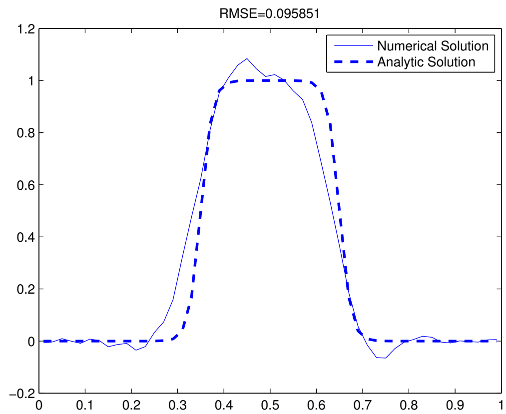

Figure 3: Second Order Accurate CGM Divergence Operator with Sixth Order Interpolation Scheme, $Cr = 1.1$.

first and last node on the boundary. However, the gradient itself is calculated at the nodes. For better understanding refer to figure (4). Now remember that in this paper, the variable q is stored only at the cell centers and not on the nodes. Hence, to solve equation (1) using CGM gradient one needs to calculate the gradient at the middle of the cells where the data exists. This leaves us with different implementation.

In the first approach, denoted as *V1*, the data is first interpolated from the cell centers to the boundary points using either linear or forth order interpolation scheme. To do so, the periodic boundary condition is also used. Once the gradient is calculated at the nodes using the CGM gradient operator, it is linearly interpolated to the cell centers. For easier understanding refer to figure (5). Hence, in V1 approach the calculated gradient is interpolated to the cell centers.

In the second approach, denoted as *V2*, it is assumed that the domain starts from the middle of the first cell and ends at the middle of the last cell. Then the data is interpolated from the cell centers to all the interior nodes. Hence, once the CGM gradient operator is applied, the gradient is calculated at the cell centers of the original grid and there is no need to interpolate the calculated gradient. For better understanding refer to figure (6). It has to be noted that in this case only higher order interpolation is possible, otherwise, the boundary conditions won't affect the solution.

The third approach, denoted as *V3*, is similar to V1, except that once the gradient is calculated at the nodes, a forth order interpolator is used to obtain the gradient at the cell centers. All methods produce a relatively smooth solution. V1's solutions

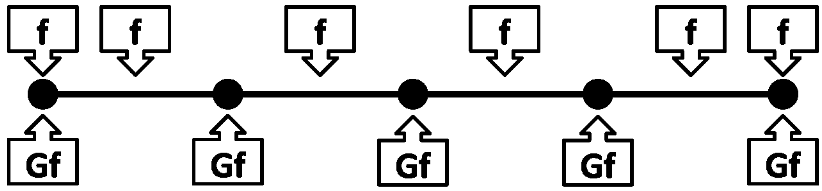

Figure 4: CGM Gradient, f denotes the locations that the data must be held and Gf shows the location where the gradient is calculated using CGM Gradient operator.

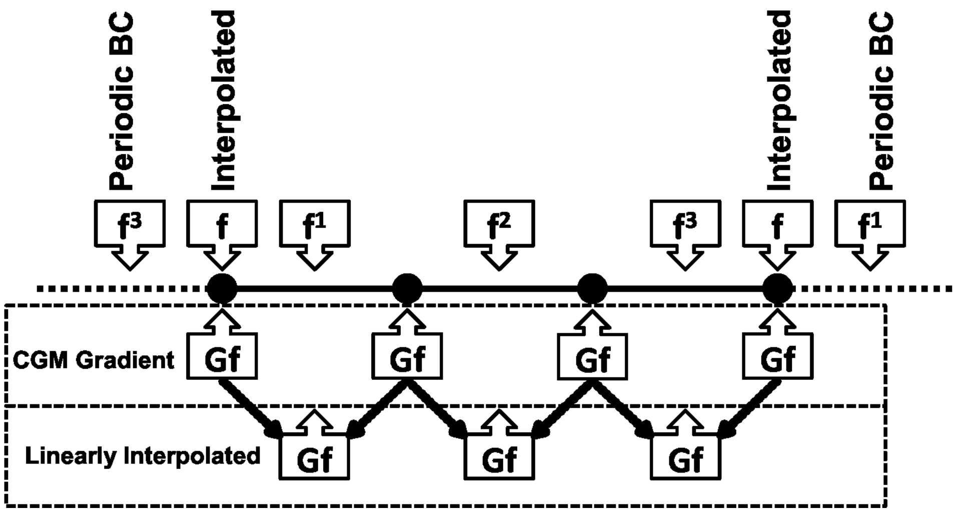

Figure 5: V1 Approach: Data is located at the cell centers only. Using the boundary condition data is interpolated at the boundary nodes to satisfy the grid requirements of the CGM gradient operator. The gradient is calculated then at the nodes and linearly interpolated to the cell centers.

shown the most error; however, it was stable upto Courant number 1.8 for both linear and forth order interpolation. V2 and V3 were both stable upto Courant number 1.3 and they were both more accurate than V1. V2 achieved less accuracy at lower Courant numbers relative to V3. Firgure (7), (8), and (9) shows sample output of different implementations.

By increasing the order of accuracy of the operators, the stable courant number decreases. However, for the forth order accurate CGM operators, the lowest stable Courant number was 1.1. Figure (10) shows the RMSE and the stable courant number of all methods compared together.

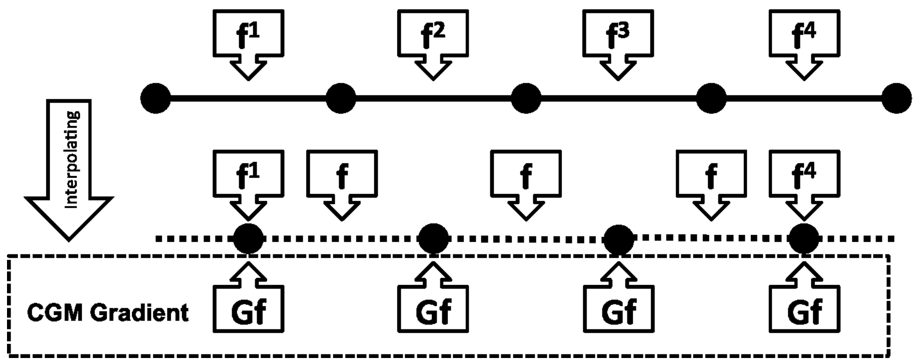

Figure 6: V2 Approach: Data is interpolated to all the interior nodes. CGM gradient operator is used to calculate the gradient at the cell centers directly. Hence, there is no need to interpolate the calculated gradient.

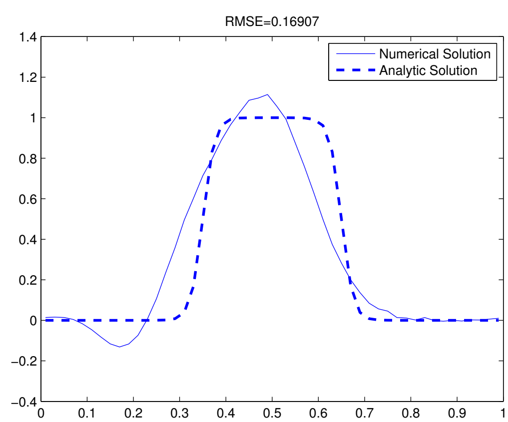

Figure 7: Second Order Accurate CGM Gradient Operator with forth Order Interpolation Scheme using V1 approach, $Cr = 1.65$.

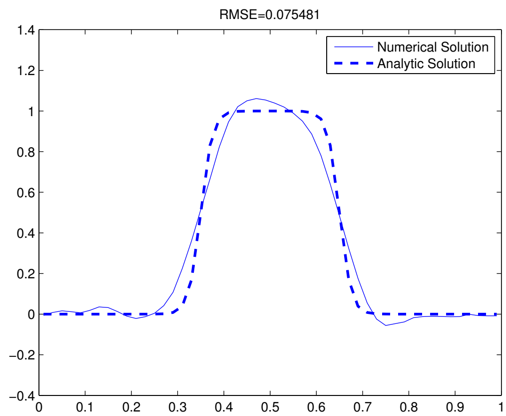

Figure 8: Second Order Accurate CGM Gradient Operator with forth Order Interpolation Scheme using V2 approach, $Cr = 1.2$.

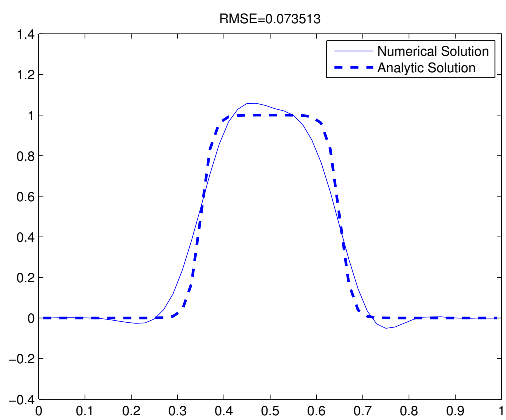

Figure 9: Second Order Accurate CGM Gradient Operator with forth Order Interpolation Scheme using V3 approach, $Cr = 1.2$.

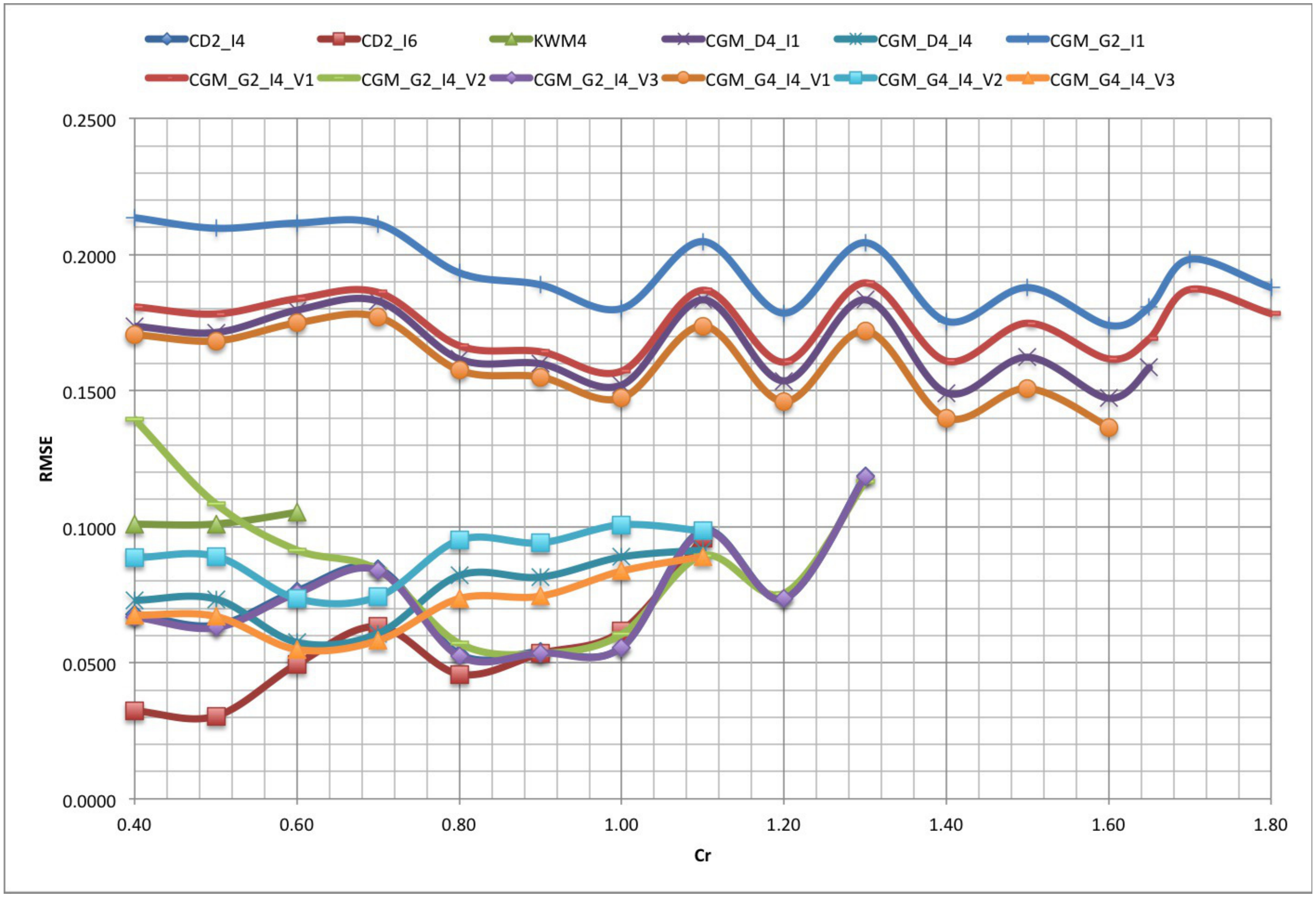

Figure 10: All methods compared together.

References

1. Marchuk, I.. Numerical Methods in Weather Prediction. 1974.
2. Mesinger, F.M.. Forward-backward scheme, and its use in a limited area model. *Contributions to atmospheric physics; Beitrage zur Physik der Atmosphare* 1977;50:200–210.
3. Klemp, J.B., Wilhelmson, R.B.. The Simulation of Three-Dimensional Convective Storm Dynamics. *Journal of the Atmospheric Sciences* 1978;35(6):1070–1096. doi:10.1175/1520-0469(1978)035¡1070:TSOTDC¿2.0.CO;2. URL `http://adsabs.harvard.edu/abs/1978JAtS...35.1070K`.
4. Tremback, C.J., Powell, J., Cotton, W.R., Pielke, R.A.. The Forwardin-Time Upstream Advection Scheme: Extension to Higher Orders. *Monthly Weather Review* 1987;115(2):540–555. doi:10.1175/1520-0493(1987).
5. Wicker, L.J., Skamarock, W.C.. A Time-Splitting Scheme for the Elastic Equations Incorporating Second-Order RungeKutta Time Differencing. *Monthly Weather Review* 1998;126(7):1992–1999. doi:10.1175/1520-0493(1998).
6. Wicker, L.J., Skamarock, W.C.. Time-Splitting Methods for Elastic Models Using Forward Time Schemes. *Monthly Weather Review* 2002;130(8):2088–2097. doi:10.1175/1520-0493(2002).
7. Abouali, M., Castillo, J.E.. Unified Curvilinear Ocean Atmosphere Model (UCOAM): A vertical velocity case study. *Mathematical and Computer Modelling* 2011;null(null). doi:10.1016/j.mcm.2011.03.023. URL `http://dx.doi.org/10.1016/j.mcm.2011.03.023` `http://linkinghub.elsevier.com/retrieve/pii/S089571771100183X`.
8. Klemp, J.B., Gill, D.O., Barker, D.M., Duda, M.G., Wang, W., Powers, J.G.. A Description of the Advanced Research WRF Version 3 2008;(June).
9. NCAR, . ARW Version 3 Modelling System User's Guide. Tech. Rep.; National Center for Atmospheric Research; 2012. URL `http://www.mmm.ucar.edu/wrf/users/pub-doc.html`.
10. Anderson, J.. Computational Fluid Dynamics. 1 ed.; McGraw-Hill Science/Engineering/Math; 1995. ISBN 0070016852.

11. Hoffmann, K.A., Chiang, S.T.. Computational Fluid Dynamics for Engineers. 2 ed.; Engineering Education System; 1993. ISBN 0962373176.

12. Ferziger, J.H., Peric, M.. Computational Methods for Fluid Dynamics. 3 ed.; Springer; 2001. ISBN 3540420746.

13. Batista, E.D., Castillo, J.E.. Mimetic Schemes on non-uniform structured meshes. *Electronic Transactions on Numerical Analysis* 2009;34:152–162.

14. Castillo, J.E., Hyman, J., Shashkov, M., Steinberg, S.. High-Order Mimetic Finite Difference Methods on Nonuniform Grids - Abstract - UK PubMed Central. ???? URL `http://ukpmc.ac.uk/abstract/CIT/70690`.

15. Castillo, J., Hyman, J., Shashkov, M., Steinberg, S.. Fourth- and sixth-order conservative finite difference approximations of the divergence and gradient. *Applied Numerical Mathematics* 2001;37(1-2):171–187. doi:10.1016/S0168-9274(00)00033-7. URL `http://dx.doi.org/10.1016/S0168-9274(00)00033-7`.

16. Castillo, J., Hyman, J., Shashkov, M., Steinberg, S.. The sensitivity and accuracy of fourth order finite-difference schemes on nonuniform grids in one dimension. *Computers & Mathematics with Applications* 1995;30(8):41–55. doi:10.1016/0898-1221(95)00136-M. URL `http://dx.doi.org/10.1016/0898-1221(95)00136-M`.

17. Castillo, J.E., Grone, R.D.. A Matrix Analysis Approach to Higher-Order Approximations for Divergence and Gradients Satisfying a Global Conservation Law. *SIAM Journal on Matrix Analysis and Applications* 2003;25(1):128–142. doi:10.1137/S0895479801398025.

18. Castillo, J.E., Yasuda, M.. Linear Systems Arising for Second-Order Mimetic Divergence and Gradient Discretizations. *Journal of Mathematical Modelling and Algorithms* 2005;4(1):67–82. doi:10.1007/s10852-004-3523-1. URL `http://www.springerlink.com/content/t2352631t340h83q/`.

19. Hernández, F., Castillo, J., Larrazábal, G.. Large sparse linear systems arising from mimetic discretization. *Computers & Mathematics with Applications* 2007;53(1):1–11. doi:10.1016/j.camwa.2006.08.034. URL `http://dx.doi.org/10.1016/j.camwa.2006.08.034`.

20. Kawamura, T., Takami, H., Kuwahara, K.. Computation of high Reynolds number flow around a circular cylinder with surface roughness. *Fluid Dynamics Research* 1986;1(2):145–162. doi:10.1016/0169-5983(86)90014-6. URL `http://stacks.iop.org/1873-7005/1/i=2/a=A05`.